



Comparative Analysis of Electrode Performance and Thermal Treatments in SMAW of Dissimilar Metal Joints

Mohammed D. Hamdey^{1*}, Ahmed Hashim Kareem², Bashar Mahmood Ali³, Muhammad Asmail Eleiwi⁴, Hasan Shakir Majdi⁵, Mohammed M. Aldabbagh⁶

¹ Department of Mechanical Engineering, College of Engineering, Al-Nahrain University, Baghdad 64040, Iraq

² Mechanical Techniques Department, Amarah Technical Institute, Southern Technical University, Basra 44001, Iraq

³ Department of Construction Engineering and Project Management, College of Engineering, Alnoor University, Mosul 41012, Iraq

⁴ Electromechanical Engineering Department, College of Engineering, University of Samarra, Samarra 34010, Iraq

⁵ Department of Chemical Engineering and Petroleum Industries, Al-Mustaqbal University College, Hillah 51001, Iraq

⁶ Power Mechanics Technology Department, Northern Technical University, Kirkuk 36001, Iraq

Corresponding Author Email: mohammed.du.hamdey@nahrainuniv.edu.iq

Copyright: ©2024 The authors. This article is published by IETA and is licensed under the CC BY 4.0 license (<http://creativecommons.org/licenses/by/4.0/>).

<https://doi.org/10.18280/ijht.420636>

ABSTRACT

Received: 29 September 2024

Revised: 26 November 2024

Accepted: 10 December 2024

Available online: 31 December 2024

Keywords:

dissimilar welding, SMAW, electrode selection, post-weld heat treatment (PWHT), weld zone microstructure

AISI 316 stainless steel and ASTM A516 alloy steel weldment characteristics investigated according to filler materials and post weld heat treatment performance. The welding was performed using shielded metal arc welding (SMAW) with two types of filler metals, E7018 and E310, and PWHT was carried out at three temperatures: 600°C, 630°C, and 650°C. Welded joints' mechanical performance encompassed tensile and bending tests, and micro-hardness measurements, in addition to microstructural and fractographical examination employed for this purpose. Results evidenced that tensile strength and elongation of welded steel using E7018 electrode were 518 MPa and 28.1%, respectively, which showed relatively high strength. The results show steel welded with E310 electrode had higher mechanical properties, with the best balance between strength and ductility. In addition, post welding heat treatment improving mechanical properties by minimizing residual stress and refining grain structure. E7018 welded joints failure load increased to 86 KN after PWHT and the ultimate tensile strength increased to 525 MPa, further, microstructure analysis of optical microscope and scanning electron microscope shows PWHT has good effect on ductility improvement and hardness reduction. New microstructures with finer grain size and increased ferrite phase observed, which enhanced tensile and bend strength.

1. INTRODUCTION

Dissimilar steel welding (DMW) among stainless steel and alloy steel gives particular demanding situations and abilities in innovative commercial packages. Stainless metallic, diagnosed for its corrosion resistance and energy, the side of alloy metal, cited for its sturdiness and machinability, is normally employed in sectors inclusive of power generation, petrochemical processing, and the automobile industry. Welding these two substances necessitates meticulous law of welding situations, choice of suitable electrode types, and publishing weld heat remedy (PWHT) application to obtain most beneficial long time mechanical residences and sturdiness. The selection of welding parameters, along with cutting-edge, voltage, and tour pace, plays essential function in warmth entry calculations, sooner or later, the best of the welded joint. Fitri et al. [1] tested modern ranges' consequences on microstructure and mechanical homes of chrome steel and alloy metallic distinctive junctions. They found that expanded present day tiers result in more heat entry,

which finally influences the volume of warmth affected quarter (HAZ) and grain shape in the weld. In comparison, Mičian et al. [2] confirmed that reduced warmth input, achieved through optimized welding modern and tour pace, affects in finer grain systems and superior mechanical properties. The significance of controlling welding parameters in SMAW modified into further emphasized using Gery et al. [3], who explored the connection between welding velocity and warmth distribution throughout the assorted joints. Their examination concluded that slow welding speeds sell immoderate heat accumulation, important to wider HAZs, and improve hazard of cracking because of extraordinary thermal growth between metals.

Electrode's composition, particularly metal filler, influences chemical composition of weld metallic and its compatibility with the base metals. Hariprasath et al. [4] conducted comprehensive study of shielded metallic arc welding (SMAW) several electrode packages across special metals. Their findings prove that nickel-primarily based electrodes, together with ENiCrFe-3, enhance the metallurgical

compatibility between stainless steel and alloy metallic by way of lowering the manufacturing of brittle intermetallic compounds on the weld interface. Likewise, El-Shennawy et al. [5] discovered that using an E309L electrode, particularly engineered for welding chrome steel with carbon or low-alloy steels, resulted in welds exhibiting more suitable toughness and corrosion resistance due to its capacity to house the thermal and chemical discrepancies between the two metals. In their evaluation, Akash et al. [6] investigated the softness of ferritic electrodes, mainly E410, in several metal welding approaches. Their research established that even though ferritic electrodes can provide suitable mechanical properties regarding strength, they may be susceptible to growing brittle phases, specifically whilst welding high-chromium stainless steels to alloy steels. The examination with the aid of Pahlawan et al. [7] emphasized the significance of equilibrating the composition of metallic filler with houses of base metals. They endorsed the usage of austenitic stainless steel electrodes in programs necessitating advanced corrosion resistance, as these electrodes provide a protecting oxide layer that stops corrosion in adverse situations. The disparity in thermal growth coefficients among stainless and alloy metallic can induce big residual traces in the weld, which, if unaddressed, can also cause cracking or untimely joint failure. Campos et al. [8] tested effects of various submit weld warmth treatment (PWHT) regimes on mechanical homes of various shielded steel arc welding (SMAW) connections among stainless steel and alloy metallic. Their studies established that submitting weld warmness treatment temperature between 600°C to 700°C considerably reduced residual stresses and improved ductility of welding joint. Influence of put up weld warmth treatment (PWHT) on microstructure of assorted welded joints turned into in addition examined through Khan et al. [9], who found that warmness treatment at increased temperatures facilitated grain boom inside warmness affected region (HAZ), ensuing more desirable sturdiness and fracture resistance. They additionally noted that (PWHT) faded hardness of weld quarter.

Garcia et al. [10] investigated (PWHT) effect in numerous welds' corrosion resistance. Their commentary concluded that (PWHT) now not handiest boosts welding area mechanical residences but also improves weld joint pitting and crevice corrosion resistance, especially with chloride ion environments. This enhancement became ascribed to the alleviation of residual tensions and the uniformity of the weld metallic. Recent studies by way of Ravi et al. [11] examined the combined impact of welding settings, electrode selection, and (PWHT) on exceptional metallic weld fatigue existence. They decided that PWHT is essential for boosting the fatigue resistance of the joint by reducing strain concentrations on the weld contact. Their findings recommend that (PWHT) should be regarded as a vital element of welding process. Microstructural changes in weld place and warmth affected area are unavoidable at some stage in many metal welding, and these adjustments notably affect joint mechanical homes. Dak and Pandey [12] did a comprehensive microstructural exam of a couple of SMAW welds related to stainless steel and alloy steel, concentrating on the development of martensitic and ferritic stages within the weld metallic. The scientists also noted that controlling warmness input at some stage in welding is important to save you from immoderate development of ferritic levels, that can undermine the weld's mechanical homes.

The significance of regulating microstructural changes at

some stage in welding became further emphasized by Li et al. [13], who examined welding pace and cooling charge effects on diverse joint microstructures. Their studies indicated that fast cooling rates, often associated with extended welding speeds, can lead to the development of undesired microstructures inclusive of bainite or martensite, which diminish the weld's persistence. In precis, the effect of the SMAW technique, electrode choice, and publish weld heat remedy vital for a hit dissimilar welding joints between stainless and alloy steel. Welding settings parameters selection at once impacts warmth entry and microstructural evolution in weld area, even as deciding on appropriate electrode ensures metallurgical compatibility and mechanical performance [14]. Post weld warmth remedy complements weld joint mechanical properties and corrosion resistance by way of assuaging residual stresses and fostering a uniform microstructure.

Dissimilar metal welding (DMW) is essential for joining carbon steels to stainless steels and many other uses in areas such as power generation, aerospace. This permits the use of synergistic characteristics like strength and corrosion endurance, where problems exist due to variations in thermal and mechanical coefficients of the base metals. Such materials' property changes include differences in melting points, thermal expansion, and microstructures can result in characteristics such as cracking and poor fusion especially in the HAZ [15]. These problems affect the strength of the joint and its ability to remain bonded; the selection of appropriate filler material is vital in overcoming them.

New developments in welding are in laser welding and gas tungsten arc welding (GTAW) have enhanced the performance of dissimilar metal joints. Razzaq et al. [16] note that by using improved filler materials and controlling the welding parameters, defects have been minimized, and weld quality improved. However, more information about how post-weld heat treatment (PWHT) could help in refining the microstructure which further relieves the residual stresses and also enhances the mechanical properties of the welds also needs to be provided.

2. EXPERIMENTAL PROCEDURE

Certain studies recommended SMAW welding as a method for various fabric joining. Distinct welding techniques, specifically shielded metal arc welding (SMAW) selected to determine stainless steel and alloy steel electrodes choosing effects in produced dissimilar welding joints. Various PWHT systems have been applied to test specimens to investigate heat treatment impact on welding joint properties. Various mechanical studies, microstructural assessments, and fractographic analyses the optimal aggregation of structures for the prevailing multiple joints. The objective of the investigation is to identify stainless steel (AISI 316) to alloy steel (ASTM A516) heterogeneous joints solution with the best welding electrodes and best heat treatment required to optimize these properties.

This investigation utilized stainless steel AISI 316 grade, which is most employed stainless steel, recognized for its superior weldability. The employed alloy metal grade is ASTM A516. This material exhibits superior machinability and suitable weldability. Table 1 delineates the chemical components and their weight percentages for ASTM A516 and AISI 316. The variations in chemical composition associated with differences in thermal and mechanical properties.

Stainless steel and alloy steel plates dimensions were 300 mm × 100 mm × 4 mm. joint placed in butt joint configuration. Owing to plates inconsistent thickness, each plate has been

beveled to form singular V-groove with 30° bevel angle. Figure 1 depicts schematic of assembled plates with the groove dimensions [17].

Table 1. Base metals alloying elements weight percentage

Contains %	Cr	Ni	C	Mn	S	P	Si	Mo	Fe
ASTM A516	0.3	0.3	0.15	1.4	0.03	0.03	0.6	---	rest
AISI 316 L	17.3	12.3	0.024	1.8	0.017	0.04	0.91	2.3	rest

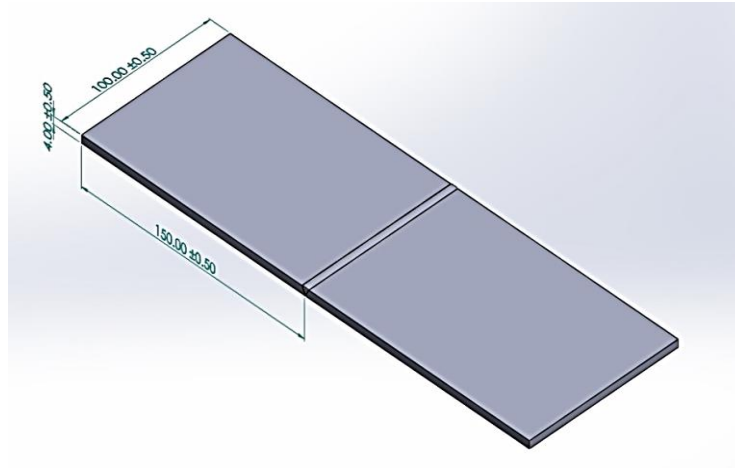


Figure 1. Plates and joint dimensions schematic

3. DISSIMILAR JOINT PARAMETERS

AISI 316 stainless steel to ASTM A516 alloy steel joining necessitates an appropriate procedure to provide defect-free and usable joints. This study utilizes shielded metallic arc welding (SMAW) methods to combine these two distinct materials. The implementation of this method will be uncomplicated for individuals seeking to work with stainless and alloy steel combinations [18]. This study employed

advanced SMAW equipment MMA 660 GT for welding processes. Results analysis includes electrode material as a variable element. Recent research has employed both E7018 and E310 as filler metals for Shielded Metal Arc Welding (SMAW). Synthetic filler rods, commercially available and conforming to AWS standards, were collected for welding applications. Table 2 illustrates chemical composition of electrode metal.

Table 2. Electrodes metal chemical composition weight percentage

Fillers	C	Mn	Si	P	S	Ni	Cr	Mo	V	Cu
E7018	0.15	1.60	0.90	0.035	0.035	0.30	0.20	0.30	0.08	---
E310	0.08	1.8	0.81	0.030	0.030	21.7	26.8	0.80	---	0.81

4. POST WELD HEAT TREATMENT (PWHT)

Welding causes changes in microstructure and elevates residual stresses in the weld metal and heat affected zone (HAZ). Tempering been utilized (PWHT) to improve characteristics of heat affected zone and weld joint. In specific experiments, (PWHT) performed 600°C for 2 hours, yielding expected characteristics [19]. Various studies utilized different experimental temperatures to examine post weld heat

treatment impact on HAZ and weld joint metals properties [20, 21]. (PWHT) of alloy steel was conducted 600°C for one hour [22]. Cooling is achieved using furnace cooling in different investigations to compare these effects in HAZ and weld joint properties [23], with studies using air-cooling techniques [23]. Three distinct temperatures employed in current study for post weld heat treatment (PWHT): 600, 630, and 650°C. Heat treatment time designated for one hour. The tested welding joints were later subjected to air-cooling.

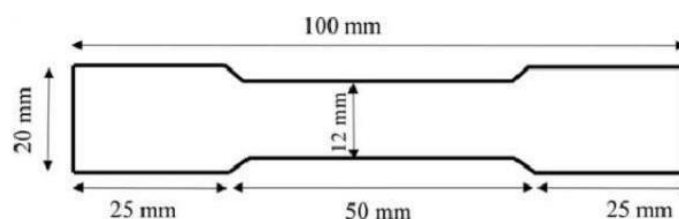


Figure 2. Schematic of the tensile test sample with dimensions

Table 3. SMAW electrode type effect on ultimate tensile strength (UTS), yield strength (YS), and elongation of stainless and alloy steel dissimilar joints

Parameters	E7018	E310
Ultimate Tensile Strength (UTS) (MPa)	518	490
Yield Strength (YS) (MPa)	217	196
Elongation %	28	20

Table 4. Dissimilar SMAW joining welding process parameters

Electrode	Dia. (mm)	Current (A)	Voltage (V)	Travel Speed (cm/min)	Passes
E7018	2.4	100	20	4	1
E310	2.4	100	20	5	1

5. TESTING METHODS

Tensile, bending, and microhardness tests are employed for the evaluations that have been conducted to determine the best welding electrode and post weld heat treatment (PWHT). A tensile test was run to determine the specimen's ultimate tensile strength (UTS), yield strength, and elongation percentage. It also indicates tested sample's ductility and brittleness. The tensile test done with 300 kN capacity AGX - T Plus universal testing machine. Following the ASTM E8M standard, the tensile specimen was produced and the analysis was carried out, as shown in Figure 2. EURO-3015 500 W CNC laser cutting machine reduced the dog bone's tensile strength. Under three-point loading circumstances, the flexural test illustrates the amount of force that is required to cause the material to undergo deformation. The bending test was utilized to ascertain the bending strain as well as the percentage of elongation that was brought about by the specimen's bending. The examination was carried out in a manner that is consistent with the ASTM D790 standard guidelines. Tensile test equipment was the standard test instrument that was utilized for the bending test. CNC laser cutting machine type EURO-4600 650 W was used to manufacture the specimen that was prepared for the bending test. The dimensions of the specimen were 120 millimeters by 12 millimeters by 4.50 millimeters. To determine the specimen's ductility and wear resistance, a micro-hardness examination was carried out. Post-weld heat treatment (PWHT) is investigated to determine whether or not it can affect the ductile characteristics of a variety of joints. Additionally, it sheds light on the reasoning for the specimen's fracture, which was caused by tensile stress in the heat-affected zone (HAZ) [24]. For this inquiry, the Ernst Rockwell hardness tester was utilized as the instrument for measuring hardness. Tensile test specimen results illustrated in Table 3.

To effectively perform welding joints, the process parameters must be determined based on the requirements for specific joining and electrode materials. Parameters utilized in current dissimilar joining presented in Table 4. All tensile test samples failed within the heat affected zone (HAZ). To ascertain reason for tensile test sample failures in HAZ, micro-hardness testing was conducted not at center of weld joint only but also in various regions of test specimen. Center of weld has been designated as 0 point. Stainless steel base metal segment designated to have effective value, while alloy steel segment designated as poor value. Hardness measurements obtained at distances of 3, 6, and 9 mm from weld center for both sides. Points 0 and 3 indicate weld joint fusion zone, point 6 represents weldment heat affected zone (HAZ), and point 9 denotes base metal.

6. MICROSTRUCTURE

The microstructural analysis of the material provides a comprehensive evaluation of grain structure and internal irregularities that lead to joint failure. Pandey identified welding joint heat treatment strategy of stainless steel 316 L and A516 steel dissimilar joint through weld specimen various sections microstructural examination [25]. Kumar et al. [26] investigated association between microstructural analysis and mechanical characteristics in PWHT process, identifying optimal approach for heterogeneous alloy steel welded joints. Utilized both optical microscopy and scanning electron microscopy (SEM) to reveal austenitic structure within welding zone and martensitic structure in heat affected zone (HAZ) investigated in earlier study [27]. Microstructural findings provide definitive rationale for tensile properties. Examination magnifies welding zone (WZ), (HAZ), base metal, and transition zone utilizing Olympus EXT 640 optical microscope and HITACHI SU3750 scanning electron microscope (SEM). Optical microscope achieved magnification of 100 and 50X, while scanning electron microscope (SEM) attained 2000X magnification that provided more detailed microstructure evaluation.

7. FRACTOGRAPHY

An analysis of fracture must be conducted to determine if failure ductile or brittle under tensile load. Fractography gained prominence in recent years because of advancements in scanning electron microscopy (SEM) [28]. A detailed examination of fracture surface can achieve with scanning electron microscope (SEM) during fractography. This perspective showcases features including dimples, river patterns, and lamellar ripping [29]. Acknowledgment is feasible, Pandey et al. institute examined samples exposed to tensile and impact tests fractography under various heat treatment conditions to assess heat treatment influence on surface morphology [25]. Different research organization employed field emission scanning electron microscope (FESEM) to examine (PWHT) effect in alloy steel welding samples produced via shielded metal arc welding (SMAW) technique fractography [30]. HITACHI scanning electron microscope employed to examine test samples fracture surface. 2000X Magnification employed to get photographs. Tensile test samples truncated to dimensions of 10 mm by 10 mm to enable fractographic analysis. Fractography evaluation renowned for its capacity to examine dimensions of dimples and river patterns, hence aiding in material's fracture pattern assessment.

8. RESULTS AND DISCUSSIONS

8.1 Welding method and electrode type effects on joint tensile test

Yield strength (YS), ultimate tensile strength (UTS), and elongation tested to evaluate welding techniques and various weld joint electrode-welding materials—examination outcomes detailed in Table 3. Tensile specimen fracture examination revealed that most failures transpired within (HAZ). Upon PWHT conclusion, HAZ region characteristics can improved. (PWHT) has been demonstrated to enhance the tensile fracture behavior of the material. Ultimate tensile strength, yield strength, and elongation values of welded joints are considerably superior to those of non-welded base metals. The basic alloy metal exhibits 640 MPa tensile strength, 260 MPa yield strength, and 17% elongation. Utilization of diverse welding techniques (SMAW) and specialist electrode metals (stainless steel and alloy steel) has led to an approximate 19.8% decrease in ultimate tensile strength (UTS) and 16.5% yield strength (YS) values relative to the base alloy steel. This reduction was accomplished following welding using stainless steel. The cost of elongation has risen by roughly 41.8% relative to the elongation of the basic alloy metal. Shielded Metal Arc Welding (SMAW) utilizing alloy metal filler rods has yielded enhanced tensile properties relative to alternative welding connections. This was established by contrasting two distinct welding techniques and electrodes with each other. Ultimate tensile strength (UTS), yield strength (YS), and elongation mean values of dissimilar stainless steel to alloy steel weld joints were 511 MPa, 214 MPa, and 25%, respectively. The values were attained through the utilization of SMAW and alloy steel filler rods to execute the welding operation.

8.2 PWHT effects in tensile test results

After being welded, specimens (PWHT) done according to three temperatures (600°C, 630°C, and 650°C), and then tensile strength tested for evaluation. SMAW joint tensile test results illustrated in Table 5. Additionally, comprehensive tensile test results include ultimate tensile strength, yield strength, and elongation, as well as the related standard deviations. A comparison has been made between tensile strength of base metal and results of evaluation of joint performance or weld efficiency [31]. Additionally, joint

efficiency presented in Table 5 at 600°C temperature, ultimate tensile, and yield stress values demonstrated improved performance during PWHT. After that, 630°C, 650°C post weld heat treatment resulted in worse strength characteristics, which were most likely caused by excessive aging and grain coarsening. Following the application of heat treatment, the percentage of elongation has increased in every single instance. When it comes to improving the tensile qualities of stainless steel to alloy steel dissimilar SMAW joints by using the alloy steel electrodes [32], post-weld heat treatment at 600°C is extremely convenient and useful. The specimen is subjected to 600°C heat treatment, which been demonstrated to increase ultimate tensile strength of stainless steel electrode joint. After being subjected to post weld heat treatment at 600°C, yield point has shown improved performance. In every case, elongation percentage increases after heat treatment have been administered. Therefore, post weld heat treatment at 600°C is suitable choice for improving tensile capabilities of stainless steel to alloy steel dissimilar SMAW joints that produced by stainless steel electrodes.

8.3 Different PWHT processes comparison based on bending test

In most bending test samples, failure occurred near (HAZ). PWHT effect in stainless steel to alloy steel dissimilar SMAW joints bending strength with alloy steel and stainless steel electrodes shown in Table 6. Maximum stress point in Table 6 reveals almost the same values without and without 600°C PWHT compared to samples treated with 630°C and 650°C in stainless steel to alloy steel dissimilar joint with alloy steel electrode, without PWHT and after 600°C PWHT, bending strength recorded 1583 MPa and 1581 MPa respectively. Table 6, shows that 600°C PWHT produced best bending strength with 1724 MPa when welding with E310 electrode.

8.4 Micrography analysis

According to the above tests results, the welding with SMAW and stainless steel electrodes in alloy steel to stainless steel dissimilar joint produced the best combination of mechanical qualities for both tensile and bending loads. To find out why post-weld heat treatment at 600°C increases tensile and bending strength, scanning electron microscopy (SEM) and pictures are studied.

Table 5. PWHT effect in stainless steel and alloy steel SMAW dissimilar joints ultimate tensile strength (UTS), yield strength (YS), and elongation

PWHT TEMP.	Joint with Alloy Steel Electrode				Joint with Stainless Steel Electrode			
	UTS (MPa)	YS (MPa)	Elongation %	Efficiency	UTS (MPa)	YS (MPa)	Elongation %	Efficiency
without	513	217	28	80.01%	490	198	20	76.5%
600°C	525	224	32	82.0%	510	204	23	79.6%
630°C	521	220	34	80.14%	483	202	27	75.4%
650°C	490	211	31	76.56%	478	200	24	74.6%

Table 6. PWHT effect on dissimilar SMAW welding joint bending strength

Welding with Alloy Steel Electrode				Welding with Stainless Steel Electrode			
without	600°C	630°C	650°C	without	600°C	630°C	650°C
1583	1581	1387	1326	1533	1724	1510	1497

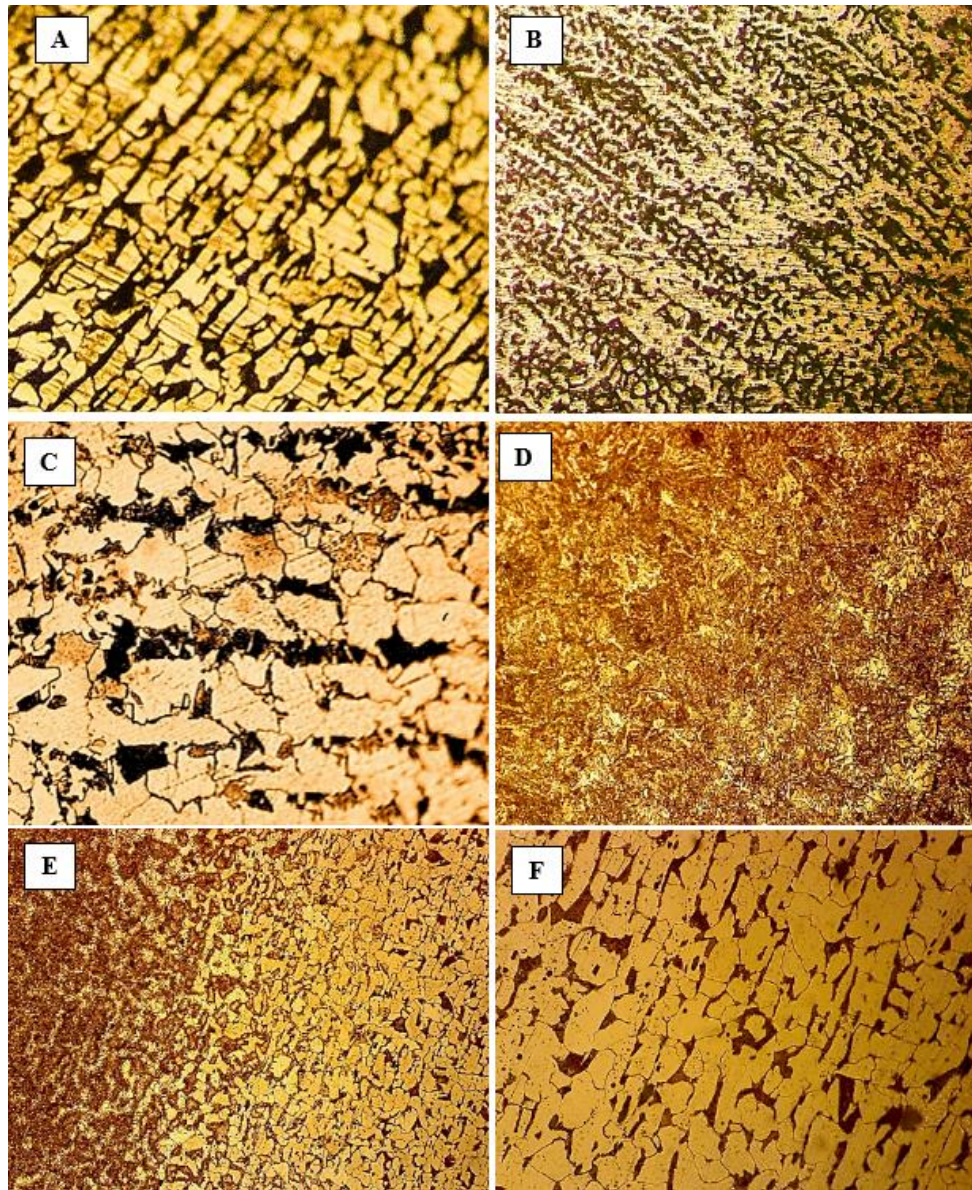


Figure 3. Optical micrographs for dissimilar SMAW welded joint with E7108 and E310 electrodes without PWHT: (A) A516 base; (B) E310 welding zone; (C) A516 HAZ; (D) E7018 welding zone; (E) stainless steel side (TZ); (F) stainless steel HAZ

8.5 Optical microstructure examination

A516 alloy steel optical micrographs depicted in Figure 3(A) reveal microstructure mostly composed of equiaxed ferrite grains and pearlite colonies, with numerous finely scattered carbides located along the ferrite grain boundaries. Occasionally, a limited number of circular MnS inclusions have been identified. (Figure 3(B)) demonstrates dissimilar E310 electrode welded joints. Lathy δ ferrite precipitates with superior grain structures seen in welding zone. The grain structure exhibited increased coarseness as optical micrography advanced toward the heat-affected zone. Partially tempered martensite and δ ferrite are also present in (HAZ). δ ferrite observed alloy steel HAZ is larger than other areas of welding joint. (Figure 3(C)) illustrates clear differential between grain size, HAZ, and weld zone δ ferrite existence. Pandey noted δ ferrite reduced amount in weld region relative to heat affected zone (HAZ) [33]. δ ferrite quantity rendered welding joint vulnerable within HAZ region [34]. Alloy steel electrode weld zone (WZ) micrograph shown in (Figure 3(D)) exhibited very large difference microstructure from E310 electrode welding zone. austenite coarse grains

transformed to low-carbon bainite/martensite or Widmanstatten ferrite structures when cooling from welding temperature with high cooling rate. When temperature much lower, fine grain size zone forms just next to coarse grain size zone. Austenite grain growth at this temperature noticed to be limited under these conditions. When cooling process continues from welding temperature, extremely fine size pearlite and ferrite grains will produced.

In this work, the dissimilar welding of A516 alloy steel with stainless steel using an E7018 electrode shows the formation of a transition zone in the stainless steel welding zone side Figure 3(E). This zone is formed from austenite with a high hardness or martensite layer as investigated in previous studies [35]. There is a group of parameters supporting the TZ formation creation in dissimilar welding of austenitic stainless steel and ferritic A516 weld metals in this work. The most important parameters that control the TZ formation are differences in chemical compositions, crystal structures, and diffusion rates between face-centered cubic (FCC) weld metal and body-centered cubic (BCC) ferritic base metal [35] other hand, high Ni content, and carbon migration phenomena will control martensite layer formation and extent inside TZ within

weld metal.

Figure 3(F) illustrates the effect of welding heat on the stainless steel HAZ for both selected welding electrodes, the increase in grain size will produce a soft zone in this region which meets the brittleness from the (TZ) and results in weak zones, for this reason, all the tensile test samples fractured in stainless steel HAZ. Optical micrographs of chosen E310 electrode SMAW welding dissimilar joint with 600°C PWHT are shown in Figure 4. After PWHT lathy ferrite structure becomes more uniform and skeletal ferrite also forms, increasing tensile strength. After 600°C PWHT, δ ferrite amount decreased in HAZ causing better mechanical properties (Figure 4(A)). Martensite amount also decreased after PWHT in HAZ which makes it less hard. Transition zone (TZ) after PWHT became more uniform compared with welding joint without PWHT as illustrated in (Figure 4(B)) which makes welded specimen stronger after PWHT. δ ferrite presence in both A516 and stainless steel HAZ became lesser which leveled up its mechanical properties.

8.6 SEM examination

SEM welding test specimen analysis provides accurate

microstructure detailed image. (Figure 5(A)), illustrate lath packets and austenite matrix with intricate details in E310 electrode weld zone due to PWHT processes. A516 HAZ portion in (Figure 5(B)) showed ferrite and pearlite mixture microstructure. Phase/constituent distribution and size are significantly heterogeneous. These microstructural results can predict higher tensile strength, hardness, and fatigue crack initiation resistance for these steels.

Stainless steel HAZ illustrated δ ferrite large amount make structure more susceptible to failure (Figure 5(C)). Stainless steel reveals cellular dendrite with δ ferrite structure, both lathy and skeletal δ ferrite amounts decreased in welding zone due to weldments PWHT, higher mechanical properties will be produced from this structure. Uniform structure bases metal less failure susceptible. Kumar et al. demonstrated that certain heat treatment procedures can alter welding zone's internal structure, while others may not have such effect [36]. Current investigation indicates that 600°C PWHT yielded satisfactory structural qualities in comparison to alternative circumstances. Welding zone TZ was similarly influenced by PWHT, resulting in better structured structure with reduced martensite and hard phases, as illustrated in Figure 5(D).

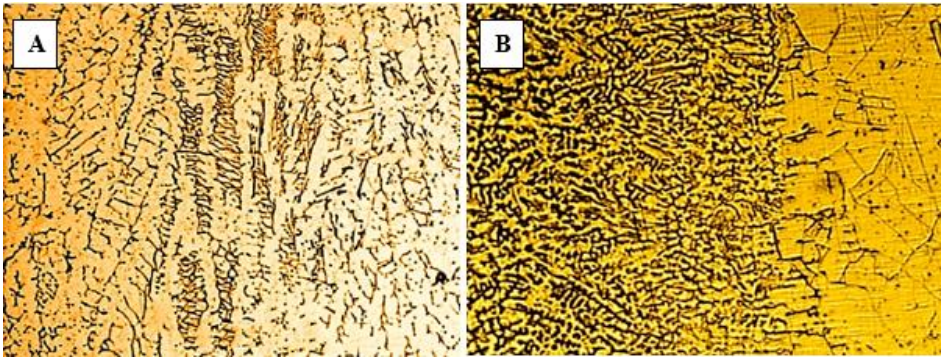


Figure 4. Dissimilar SMAW welded joint with E310 electrode after 600°C PWHT optical micrographs: (A) welding zone; (B) HAZ and TZ

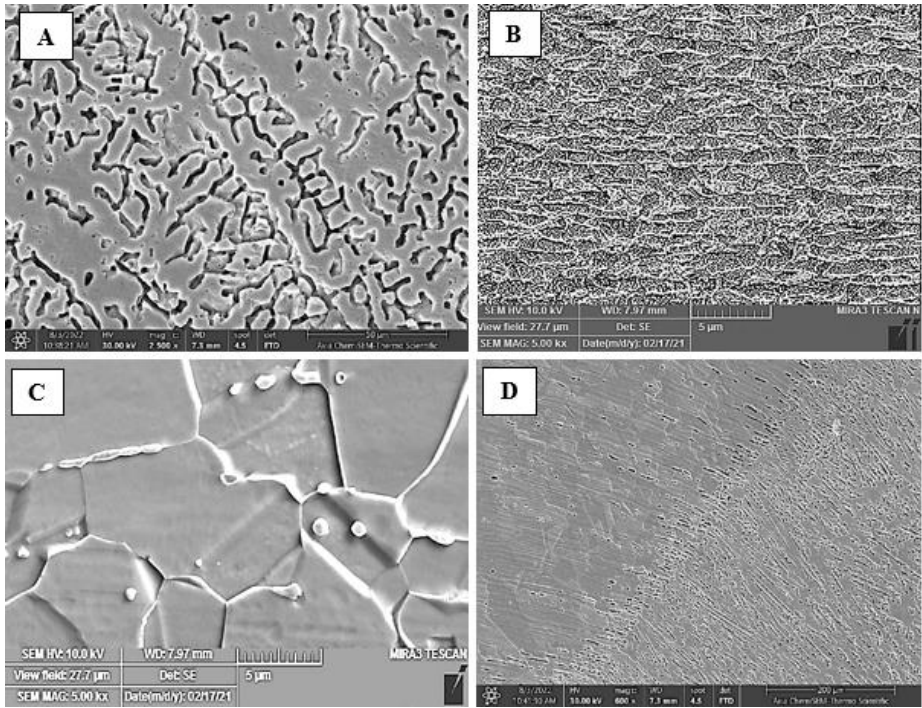


Figure 5. Dissimilar SMAW welded joint with E310 electrode and 600°C PWHT SEM image: (A) E310 welding zone; (B) A516 HAZ; (C) stainless steel HAZ; (D) transition zone

8.7 Analyzing the hardness values

Failure point's position under tensile stress can accurately determine using microhardness measurements. To ascertain actual influence of hardness in distinct region of weld joint, authors chosen multiple locations from weld specimen, encompassing fusion zone and heat affected zone. These findings consistent across all heat treatment conditions [37]. Pandey et al. found that hardness values in P91 steel pipe varied across multiple welding zones [37]. Welded P92 steel specimen heat treatment may modify hardness levels, as indicated by different studies [38]. This inquiry involved weldment microhardness testing several sections. Figure 6(A) illustrates (PWHT) effect in stainless and alloy steel dissimilar (SMAW) joint utilizing E7018 electrode microhardness. Hardness value maximal in weld zone region, as previously observed. On both weld zone sides, known as (HAZ), it diminishes by 3 to 9 millimeters. This location was weakness points in all tensile tested samples. In most cases, hardness value is elevated in vicinity of weldment as well. Martensitic structure has developed in weld zone, enhancing its toughness. One method to mitigate this through PWHT application. weldment hardness values diminished following 600°C post weld heat treatment comparison to as welded condition to evaluate the heat treatment effects. Figure 6(B) illustrates (PWHT) impact in dissimilar stainless steel and alloy steel E310 electrodes (SMAW) joints microhardness. Ideal approach for SMAW utilizing E310 electrode. Regarding tensile and bending tests after 600°C post weld heat treatment for both electrodes, reduction from 35.2 to 32.4 HRC (Figure 6(A)) and from 35.2 to 34.6 HRC (Figure 6(B)) in hardness

values in weld zone observed. Elongation during tensile test increases as hardness values decrease after post weld heat treatment (PWHT). Zones affected by heat exhibit lowest hardness ratings and more susceptible to tensile failure. PWHT procedure selected for SMAW process based on hardness values.

8.8 Fracture pattern from fractography

Base alloy steel and stainless steel SEM fractography shown in Figure 7(A) and Figure 7(B). In alloy steel case Figure 7(A), fracture will propagate in grain boundaries. Welding joint and HAZ ductility show less severity in A516 fracture section and it shows less elongation amount, in Figure 7(B), considerable dimples number found in stainless steel fractography. So, elongation will be large in AISI 316 stainless steel, and more ductile fracture. E7018 electrode joint illustrated dimple structures in specimens with and without PWHT. Figure 7(C), shows test specimen fractography without heat treatment, fine size dimples produced from lamellar tearing occur in this zone. Figure 7(D), after 600°C PWHT illustrates large dimple size produced plasticity with value larger than welding joints without heat treatment. Figure 7(E), illustrates E310 electrode welding joint without heat treatment with cleavage fracture which is kind of trans-granular brittle fracture. Crack propagation creates river like pattern in cleavage fracture. In Figure 7(F), intergranular fracture founded in specimen with 600°C PWHT. This fracture type shows ductile characteristics and fine size dimples related to grain refinement, which indicates larger plasticity and elongation.

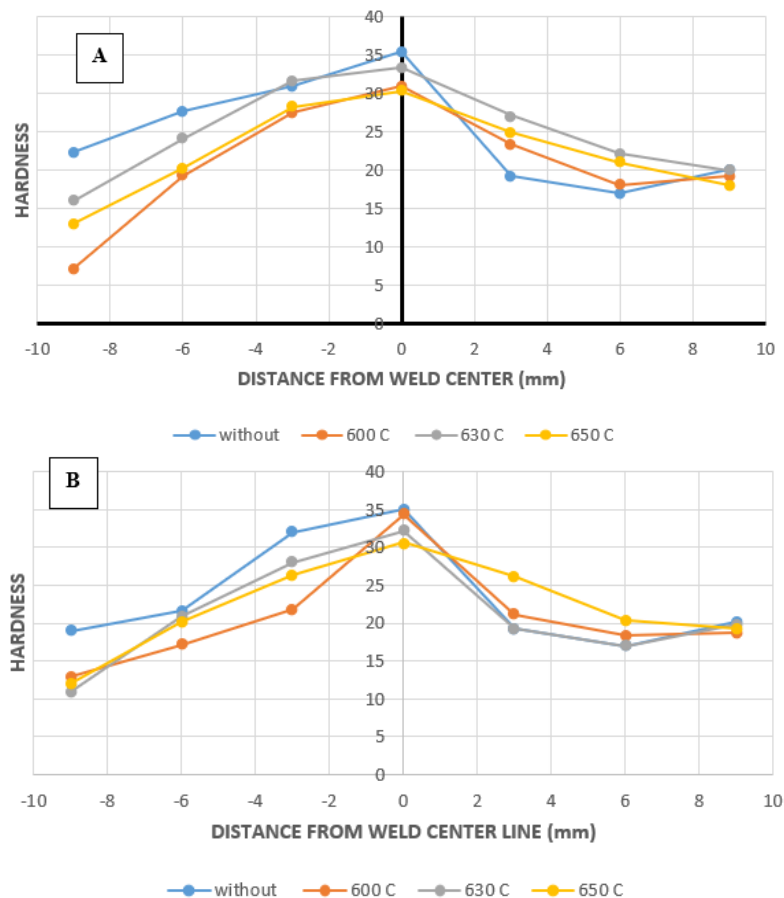


Figure 6. Weldment hardness profile: (A) SMAW joint with E7018 electrode microhardness profile; (B) SMAW joint with E310 electrode microhardness

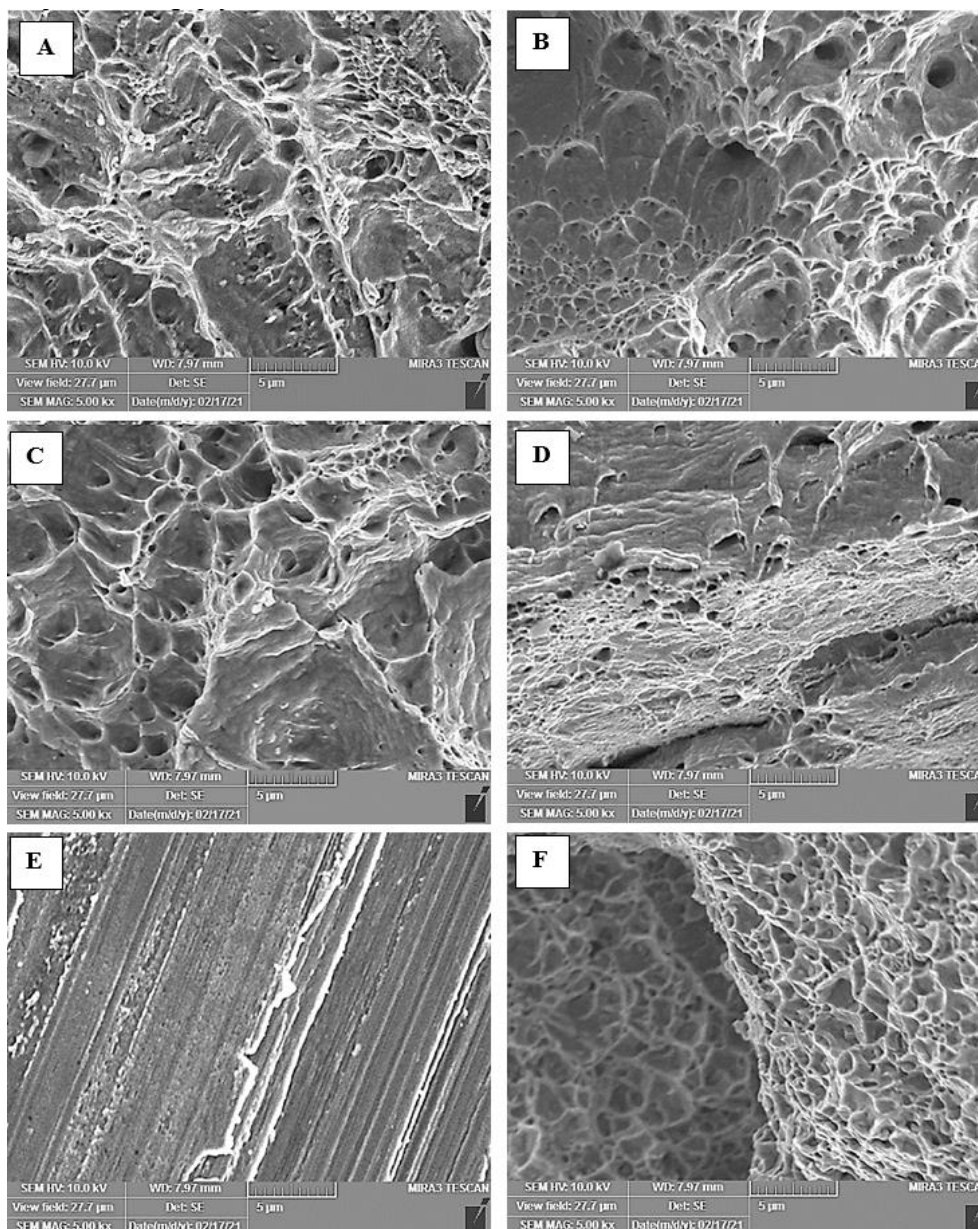


Figure 7. SEM fractography: (A) alloy steel base metal fractography; (B) stainless steel base metal fractography; (C) E7018 welding joint without heat treatment fractography; (D) E7108 welding joint with 600°C heat treatment fractography; (E) E310 welding joint without heat treatment fractography; (F) E310 welding joint with 600°C heat treatment fractography

9. COMPARISON OF USED ELECTRODES AND HEAT TREATMENTS EFFECTS ON MECHANICAL PROPERTIES

From the tested specimens that were welded with E7018 electrodes, it obtained an average of the ultimate tensile strength of 518 MPa and percentage elongation of 28%. This suggests moderately high weld strength though there was information in terms of ductility and other overall weld qualities. MMA EL E310 tested for Welding performance did result in better increase in qualitative characteristics of the welded joints than the E7018. Tensile strength and ductility, consequently, overall joint efficiency was increased. PWHT at 600°C introduced an additional improvement in the mechanical properties compared to the base metal to increase the property to a highest value of 525 MPa in UTS levels and also in minimizing the levels of residual stress. The results also showed that from the heat treatment, we get better

microstructure and enhancement of tensile and bending strength. However, the rise of heat treatment temperature to 630°C and 650°C helped enhance general characteristics of the joined materials. The tensile strength was being increased beyond the set point, while the hardness felt down, especially at the HAZ. These treatments decreased the brittleness of the welded joints and increased the ductility over the base welded joints. Apart from raising the ferrite amount at the higher temperature, heat treatment favored the microstructure by revealing better grain refinement. This microstructural improvement contributed into achieving superior tensile and bending strength compared with the area of the welded joints and particularly for the material that was subjected to the temperature of 650°C. SEM and Optical Microscopy analysis confirmed that despite having undergone the PWHT the desired fine grain structures are still present in the welds and these Microstructures are held responsible for improving both strength and ductility of welded joints.

10. CONCLUSIONS

This study provides a thorough assessment of the Shielded Metal Arc Welding (SMAW) process applied to various joints of AISI 316 stainless steel and ASTM A516 alloy steel. The study highlights the essential importance of electrode selection, welding conditions, and (PWHT) in enhancing welded joints' mechanical properties and microstructure.

1. The findings indicate that the usage of chrome steel-based total electrodes, like the E310, extensively complements the metallurgical compatibility of chrome steel and alloy metallic joints. This is usually attributed to the discount of brittle intermetallic compound manufacturing, which right away enhances the power and corrosion resistance of the welded interface. The E310 electrode has established the capability to house temperature and chemical versions across base metals, enhancing weld integrity.
2. The PWHT software, especially at 600°C, is critical for diminishing residual stresses, enhancing ductility, and fostering consistent grain systems in (HAZ). Microstructural evaluation discovered that PWHT promoted grain growth and the alternate ferritic and martensitic stages, resulting in more suitable sturdiness and fracture resistance. The thermal treatment also caused stronger tensile electricity, elongation, and bending strength, illustrating the effectiveness of submit-weld thermal manipulation.
3. Furthermore, the observation demonstrates the effect of controlled heat entry and welding speed on the microstructural evolution of the weld area. Excessive thermal input is associated with the production of broader HAZ regions and undesirable microstructures, such as martensite, which can also jeopardize joint durability. Consequently, specific control of welding conditions is critical for accomplishing advanced mechanical characteristics and decreasing the likelihood of weld failure.
4. This analysis underscores that the combination of most desirable electrode choice and publish-weld warmth treatment is essential for producing exceptional, long lasting metallic welds. Specifically, post-weld warmth treatment at six hundred stages Celsius always more desirable overall performance via strengthening both tensile and bending strengths and promoting microstructural homogeneity. These discoveries offer enormous sensible effects for business applications necessitating specialized metallic welding, appreciably in electricity producing, petrochemical processing, and car manufacturing industries.
5. Future studies may additionally check out the long-term period performance of welded joints beneath numerous climatic and mechanical instances, as well as the capacity for in addition refining post-weld warmth remedy regimens and welding parameters to beautify mechanical efficiency.

11. POSSIBLE IMPLICATIONS AND FURTHER RESEARCH

The implications of the findings from this research on dissimilar metal welding (DMW) using E7018 and E310 electrodes, and the effects of post-weld heat treatment

(PWHT) have the following practical usefulness in differing materials joining industries, note: Areas in which such research can be utilized include power sector, aerospace manufacturing, chemical and nuclear manufacturing, construction and heavy engineering industries among others. Based on the current study, there are some possible directions for future research to better understand and enhance DMW performance, including the comparison of other alloys for DMW, that exceed E7018 and E310, such as Ni-based or Cu-added filler metals. Furthermore, in the current study, the PWHT was done at the three fixed temperatures of 600°C, 630°C and 650°C. These may comprise the effect of cooling rates or temperature profiles, that is rate of temperature increase and decrease on properties of the DMW joints, and its fatigue characteristics and durability in cyclic loadings and fluctuating high temperatures. Thus, the areas that accelerated life-cycle testing can help in analyzing the behavior of welded joints under realistic conditions including nuclear reactors, aircraft, and spacecraft construction.

REFERENCES

- [1] Fitri, M., Hidayatulloh, P., Wibowo, K.M., Darmawan, A.S. (2021). The effect of smaw welding currents on mechanical properties and micro structures of low carbon steels. *Materials Science Forum*, 1029: 15-23. <https://doi.org/10.4028/www.scientific.net/MSF.1029.15>
- [2] Mičian, M., Frátrik, M., Kajánek, D. (2021). Influence of welding parameters and filler material on the mechanical properties of HSLA steel S960MC welded joints. *Metals*, 11(2): 305. <https://doi.org/10.3390/met11020305>
- [3] Gery, D., Long, H., Maropoulos, P. (2005). Effects of welding speed, energy input and heat source distribution on temperature variations in butt joint welding. *Journal of Materials Processing Technology*, 167(2-3): 393-401. <https://doi.org/10.1016/j.jmatprotec.2005.06.018>
- [4] Hariprasath, P., Sivaraj, P., Balasubramanian, V., Pilli, S., Sridhar, K. (2022). Effect of the welding technique on mechanical properties and metallurgical characteristics of the naval grade high strength low alloy steel joints produced by SMAW and GMAW. *CIRP Journal of Manufacturing Science and Technology*, 37: 584-595, <https://doi.org/10.1016/j.cirpj.2022.03.007>
- [5] El-Shennawy, M., Abdel-Aleem, H.A., Ghanem, M.M., Sehsah, A.M. (2024). Effect of welding parameters on microstructure and mechanical properties of dissimilar AISI 304/ductile cast iron fusion welded joints. *Scientific Reports*, 14(1): 19827. <https://doi.org/10.1038/s41598-024-70050-0>
- [6] Akash, G., Prashant, K., Upinder, K., Vishaldeep, S. (2019). Investigation of mechanical strength and material characterization on disparate TIG-welded joints of ferrous alloys. *Think India Journal*, 22(17).
- [7] Pahlawan, I.A., Arifin, A.A., Marliana, E. (2021). Effect of welding electrode variation on dissimilar metal weld of 316L stainless steel and steel ST41. *IOP Conference Series: Materials Science and Engineering*, 1010(1): 012001. <https://doi.org/10.1088/1757-899X/1010/1/012001>
- [8] Campos, W.R.C., Ribeiro, V.S., Vilela, A.H.F., Almeida, C.R.O. (2017). Effects of post-weld heat treatment and weld overlay on the residual stress and mechanical

- properties in dissimilar metal weld. International Nuclear Information System.
- [9] Khan, M., Dewan, M.W., Sarkar, M.Z. (2021). Effects of welding technique, filler metal, and post-weld heat treatment on stainless steel and mild steel dissimilar welding joint. *Journal of Manufacturing Processes*, 64: 1307-1321. <https://doi.org/10.1016/j.jmapro.2021.02.058>
 - [10] Garcia, J.H.N., Santos, N.F., Esteves, L. (2019). Corrosion behavior of 316L and Alloy 182 dissimilar weld joint with post-weld heat treatment. *Matéria (Rio de Janeiro)*, 24(3): e12141. <https://doi.org/10.1590/S1517-707620190003.0787>
 - [11] Ravi, S., Balasubramanian, V., Nasser, S.N. (2005). Influences of post-weld heat treatment on fatigue life prediction of strength mismatched HSLA steel welds. *International Journal of Fatigue*, 27(5): 547-553. <https://doi.org/10.1016/j.ijfatigue.2004.09.006>
 - [12] Dak, G., Pandey, C. (2020). A critical review on dissimilar welds joint between martensitic and austenitic steel for power plant application. *Journal of Manufacturing Processes*, 58: 377-406. <https://doi.org/10.1016/j.jmapro.2020.08.019>
 - [13] Li, Z., Yu, G., He, X., Li, S., Zhao, Y. (2018). Numerical and experimental investigations of solidification parameters and mechanical property during laser dissimilar welding. *Metals*, 8(10): 799. <https://doi.org/10.3390/met8100799>
 - [14] Kumar, R., Varma, A., Kumar, Y.R., Neelakantan, S. (2022). Enhancement of mechanical properties through modified post-weld heat treatment processes of T91 and Super304H dissimilar welded joint. *Journal of Manufacturing Processes*, 78: 59-70. <https://doi.org/10.1016/j.jmapro.2022.04.008>
 - [15] Sun, Z., Ion, J.C. (1995). Laser welding of dissimilar metal combinations. *Journal of Materials Science*, 30: 4205-4214. <https://doi.org/10.1007/BF00361499>
 - [16] Razzaq, S., Pan, Z.X., Li, H.J., Ringer, S.P., Liao, X.Z. (2024). Joining dissimilar metals by additive manufacturing: A review. *Journal of Materials Science & Technology*, 31: 2820-2845. <https://doi.org/10.1016/j.jmrt.2024.07.033>
 - [17] Lincoln Electric Company. (2003). *The Procedure Handbook of Arc Welding* (14th Ed.). James F Lincoln. <https://www.scribd.com/doc/206230320/The-Lincoln-Procedure-Handbook-of-Arc-Welding>.
 - [18] Dauod, D.S., Wade, K.J., Mohammed, M.S., Majdi, H.S. (2024). Analysis of shielding gases influences 304 gas metal arc welding microstructure, weld geometry, and mechanical properties. *Revue des Composites et des Matériaux Avancés*, 34(4): 435-446. <https://doi.org/10.18280/rcma.340405>
 - [19] Zhang, J., Huang, Y., Fan, D., Zhao, J., Huang, J., Yu, X., Liu, S. (2020). Microstructure and performances of dissimilar joints between 12Cr2Mo1R steel and 06Cr18Ni11Ti austenitic stainless steel joined by AA-TIG welding. *Journal of Manufacturing Processes*, 60: 96-106. <https://doi.org/10.1016/j.jmapro.2020.10.048>
 - [20] Joseph, A., Rai, S.K., Jayakumar, T., Murugan, N. (2005). Evaluation of residual stresses in dissimilar weld joints. *International Journal of Pressure Vessels and Piping*, 82(9): 700-705. <https://doi.org/10.1016/j.ijpvp.2005.03.006>
 - [21] Chenna Krishna, S., Srinath, J., Jha, A.K., Pant, B., Sharma, S.C., George, K.M. (2013). Effect of heat treatment on microstructure and mechanical properties of 12Cr-10Ni-0.25 Ti-0.7 Mo stainless steel. *Metallography, Microstructure, and Analysis*, 2: 234-241. <https://doi.org/10.1007/s13632-013-0079-3>
 - [22] Sharma, C., Dwivedi, D.K., Kumar, P. (2013). Effect of post weld heat treatments on microstructure and mechanical properties of friction stir welded joints of Al-Zn-Mg alloy AA7039. *Materials & Design*, 43: 134-143. <https://doi.org/10.1016/j.matdes.2012.06.018>
 - [23] Dewan, M.W., Liang, J., Wahab, M.A., Okeil, A.M. (2014). Effect of post-weld heat treatment and electrolytic plasma processing on tungsten inert gas welded AISI 4140 alloy steel. *Materials & Design* (1980-2015), 54: 6-13. <https://doi.org/10.1016/j.matdes.2013.08.035>
 - [24] Paventhan, R., Lakshminarayanan, P.R., Balasubramanian, V. (2011). Fatigue behaviour of friction welded medium carbon steel and austenitic stainless steel dissimilar joints. *Materials & Design*, 32(4): 1888-1894. <https://doi.org/10.1016/j.matdes.2010.12.011>
 - [25] Thakare, J.G., Pandey, C., Mahapatra, M.M., Mulik, R.S. (2019). An assessment for mechanical and microstructure behavior of dissimilar material welded joint between nuclear grade martensitic P91 and austenitic SS304 L steel. *Journal of Manufacturing Processes*, 48: 249-259. <https://doi.org/10.1016/j.jmapro.2019.10.002>
 - [26] Pandey, C., Mahapatra, M.M., Kumar, P., Daniel, F., Adhithan, B. (2019). Softening mechanism of P91 steel weldments using heat treatments. *Archives of Civil and Mechanical Engineering*, 19: 297-310. <https://doi.org/10.1016/j.acme.2018.10.005>
 - [27] Mohamed, M.S., Abtan, A.A., Moosa, A.U. (2023). Microstructure and mechanical properties assessments of 304 austenitic stainless steel and monel 400 dissimilar GTAW weldment. *Revue des Composites et des Matériaux Avancés*, 33(3): 135-144. <https://doi.org/10.18280/rcma.330301>
 - [28] Ramkumar, K.D., Singh, A., Raghuvanshi, S., Bajpai, A., Solanki, T., Arivarasu, M., Narayanan, S. (2015). Metallurgical and mechanical characterization of dissimilar welds of austenitic stainless steel and superduplex stainless steel—A comparative study. *Journal of Manufacturing Processes*, 19: 212-232. <https://doi.org/10.1016/j.jmapro.2015.04.005>
 - [29] Shao, Q., Shi, Y., Wang, X., Li, M., Chang, Y., Gan, Y., Zhang, F. (2023). Study of repair welding on microstructure, mechanical properties and corrosion resistance of dissimilar welded joints of SUS304 and Q345B steel. *Journal of Materials Processing Technology*, 23: 4173-4189. <https://doi.org/10.1016/j.jmrt.2023.02.061>
 - [30] Wang, S., Ma, Q., Li, Y. (2011). Characterization of microstructure, mechanical properties and corrosion resistance of dissimilar welded joint between 2205 duplex stainless steel and 16MnR. *Materials & Design*, 32(2): 831-837. <https://doi.org/10.1016/j.matdes.2010.07.012>
 - [31] Mohammed, M.S., Hamdey, M.D., Kareem, A.H., Majdi, H.S. (2024). Investigation of copper backing plate effects in stainless steel welding distortion, heat distribution, and residual stress. *International Journal of Heat &*

- Technology, 42(4): 1434-1446.
<https://doi.org/10.18280/ijht.420433>
- [32] Khamouli, F., Zidani, M., Farh, H., Saoudi, A., Atoui, L. (2016). Effects of cellulosic and basic flux on the structure, composition and hardness of SMAW welds on steel X42. *International Journal of Engineering Research in Africa*, 27: 11-19.
<https://doi.org/10.4028/www.scientific.net/jera.27.11>
- [33] Dauod, D.S., Mohammed, M.S., Aziz, I.A., Abbas, A.S. (2023). Mechanical vibration influence in microstructural alterations and mechanical properties of 304 stainless steel weld joints. *Journal of Engineering Science and Technology*, 33-54.
- [34] Voigt, A.L., da Cunha, T.V., Niño, C.E. (2020). Conception, implementation and evaluation of induction wire heating system applied to hot wire GTAW (IHW-GTAW). *Journal of Materials Processing Technology*, 281: 116615.
<https://doi.org/10.1016/j.jmatprotec.2020.116615>
- [35] Ramkumar, K.D., Arivazhagan, N., Narayanan, S. (2012). Effect of filler materials on the performance of gas tungsten arc welded AISI 304 and Monel 400. *Materials & Design*, 40: 70-79.
<https://doi.org/10.1016/j.matdes.2012.03.024>
- [36] Gunasekaran, K., Solomon, I., Skvireckas, R., Dundulis, G. (2023). Influence of temperature variance on the mechanical properties of a welded bearing support flange under transient conditions using finite element approach. *Mechanics*, 29(3): 188-193.
<https://doi.org/10.5755/j02.mech.31209>
- [37] Okano, S., Mochizuki, M. (2017). Transient distortion behavior during TIG welding of thin steel plate. *Journal of Materials Processing Technology*, 241: 103-111.
<https://doi.org/10.1016/j.jmatprotec.2016.11.006>
- [38] Ghorbani, S., Ghasemi, R., Ebrahimi-Kahrizsangi, R., Hojjati-Najafabadi, A. (2017). Effect of post weld heat treatment (PWHT) on the microstructure, mechanical properties, and corrosion resistance of dissimilar stainless steels. *Materials Science and Engineering: A*, 688: 470-479.
<https://doi.org/10.1016/j.msea.2017.02.020>